Brief Communication

MOLECULAR METABOLISM

In vivo metabolic effects after acute activation of skeletal muscle G_s signaling

Jaroslawna Meister [1,], Derek B.J. Bone [1], Jonas R. Knudsen [2], Luiz F. Barella [1], Liu Liu [1], Regina Lee [1], Oksana Gavrilova [3], Min Chen [4], Lee S. Weinstein [4], Maximilian Kleinert [2,5], Thomas E. Jensen [2], Jürgen Wess [1,6,*]**

ABSTRACT

Objective: The goal of this study was to determine the glucometabolic effects of acute activation of G_s signaling in skeletal muscle (SKM) *in vivo* and its contribution to whole-body glucose homeostasis.

Methods: To address this question, we studied mice that express a G_s-coupled designer G protein-coupled receptor (Gs-DREADD or GsD) selectively in skeletal muscle. We also identified two G_s-coupled GPCRs that are endogenously expressed by SKM at relatively high levels (β_2-adrenergic receptor and CRF_2 receptor) and studied the acute metabolic effects of activating these receptors *in vivo* by highly selective agonists (clenbuterol and urocortin 2 (UCN2), respectively).

Results: Acute stimulation of GsD signaling in SKM impaired glucose tolerance in lean and obese mice by decreasing glucose uptake selectively into SKM. The acute metabolic effects following agonist activation of β_2-adrenergic and, potentially, CRF_2 receptors appear primarily mediated by altered insulin release. Clenbuterol injection improved glucose tolerance by increasing insulin secretion in lean mice. In SKM, clenbuterol stimulated glycogen breakdown. UCN2 injection resulted in decreased glucose tolerance associated with lower plasma insulin levels. The acute metabolic effects of UCN2 were not mediated by SKM G_s signaling.

Conclusions: Selective activation of G_s signaling in SKM causes an acute increase in blood glucose levels. However, acute *in vivo* stimulation of endogenous G_s-coupled receptors enriched in SKM has only a limited impact on whole-body glucose homeostasis, most likely due to the fact that these receptors are also expressed by pancreatic islets where they modulate insulin release.

Keywords Skeletal muscle; GPCR; G protein; DREADD; Clenbuterol; Urocortin 2; Glucose homeostasis

1. INTRODUCTION

G protein-coupled receptors (GPCRs) represent the largest group of cell membrane receptors. Considering the large repertoire of ligands that act through GPCRs, it is not surprising that GPCRs are involved in nearly all physiological functions in the human body. This includes regulation of food intake, insulin secretion, lipid storage, and tissue glucose uptake [1], all processes that are highly relevant in the study of metabolic disorders. It is very difficult to assess the *in vivo* metabolic functions of a specific GPCR expressed by a particular tissue or cell type, primarily because each GPCR is expressed in many organs or tissues and may be able to activate more than one class of heterotrimeric G proteins.

During the past decade, DREADD (Designer Receptor Exclusively Activated by Designer Drugs) technology [2,3] has emerged as a powerful chemogenetic tool to study the *in vivo* physiological relevance of GPCR-dependent pathways in a temporally and spatially controlled manner [1,4]. The most commonly used DREADDs are mutant muscarinic acetylcholine receptors that can be selectively activated by clozapine-N-oxide (CNO) [2,3] or certain CNO derivates such as deschloroclozapine (DCZ) [5] and compound 21 (C21) [6]. When used in the proper concentration or dose range, CNO is otherwise pharmacologically inert. During the past 15 years, DREADDs that are selectively linked to each of the four major G protein families (G_s, G_q, G_i, and G_{12}) have been developed [7].

Since SKM is responsible for the majority of insulin-mediated glucose disposal, SKM plays an important role in regulating glucose homeostasis [8]. Impaired SKM insulin sensitivity represents a key metabolic defect in the pathogenesis of type 2 diabetes [8]. An improved understanding of SKM physiology may lead to the development of novel classes of antidiabetic drugs specifically targeting SKM.

[1]Molecular Signaling Section, Laboratory of Bioorganic Chemistry, National Institute of Diabetes and Digestive and Kidney Diseases, Bethesda, MD 20892, USA [2]Department of Nutrition, Exercise and Sports, University of Copenhagen, Denmark [3]Mouse Metabolism Core, National Institute of Diabetes and Digestive and Kidney Diseases, Bethesda, MD 20892, USA [4]Metabolic Diseases Branch, National Institute of Diabetes and Digestive and Kidney Diseases, Bethesda, MD, USA [5]Muscle Physiology and Metabolism Group, German Institute of Human Nutrition Potsdam—Rehbruecke, Nuthetal, Germany [6]Laboratory of Bioorganic Chemistry, Molecular Signaling Section, National Institute of Diabetes and Digestive and Kidney Diseases, Bldg. 8A, Room B1A-05, 8 Center Drive, Bethesda, MD 20892, USA

*Corresponding author. Laboratory of Bioorganic Chemistry, Molecular Signaling Section, National Institute of Diabetes and Digestive and Kidney Diseases, Bldg. 8A, Room B1A-05, 8 Center Drive, Bethesda, MD 20892, USA. E-mail: jurgenw@niddk.nih.gov (J. Wess).

**Corresponding author. E-mail: meister.jaro@gmail.com (J. Meister).

Received August 8, 2021 • Revision received November 21, 2021 • Accepted December 2, 2021 • Available online 6 December 2021

https://doi.org/10.1016/j.molmet.2021.101415

SKM expresses dozens of GPCRs that differ in their G protein-coupling properties [9]. We have shown that activation of SKM G_q-coupled receptors has a beneficial effect on whole-body glucose homeostasis by promoting glucose uptake into SKM [10].

In this study, we explored the *in vivo* metabolic effects caused by acute activation of SKM G_s-coupled receptors. Analysis of mutant mice that expressed a G_s-coupled DREADD (Gs DREADD, hereafter GsD) selectively in SKM (SKM-GsD mice) showed that acute stimulation of G_s signaling in SKM *in vivo* impairs glucose tolerance by decreasing glucose uptake into SKM. In parallel, we used selective agonists to stimulate β_2-adrenoceptors (β_2-AR) and the corticotropin releasing hormone receptor 2 (CRF_2), two receptors that are expressed at relatively high levels in SKM. We found that acute *in vivo* stimulation of these receptors did not mimic the metabolic effects observed in CNO-treated SKM-GsD mice, most likely due to the ability of these receptors to regulate hormone secretion from pancreatic islets.

Our study provides an excellent example of how tissue expression patterns of receptors can affect the acute effects of GPCR agonists on whole-body glucose homeostasis.

2. METHODS

2.1. Mouse maintenance and diet

All mice were fed *ad libitum* and kept on a 12-h light/12-h dark cycle at room temperature (23 °C). Mice were maintained either on a standard mouse chow (7022 NIH-07 diet, 15% kcal fat, energy density 3.1 kcal/g, Envigo Inc.) or a high-fat diet (HFD, 60% kcal fat; #F3282, Bioserv). Transgenic mouse models received HFD after tamoxifen induction at the age of 10 weeks for a duration of at least 8 weeks. Lean (#B6-M, C57BL/6NTac) and obese (#DIO-B6-M, C57BL/6NTac, >8 weeks of HFD starting at the age of 6 weeks) WT mice were purchased from Taconic. Metabolic tests with mice fed standard chow were performed starting at the age of 10 weeks. Mice consuming HFD underwent metabolic tests starting at the age of 14 weeks (C57BL/6NTac WT mice) or 18 weeks (transgenic mice), respectively. All experiments were approved by the NIDDK Institutional Animal Care and Use Committee.

2.2. Generation of SKM-specific knock-out and knock-in mice

To generate SKM-specific knock-out (KO) mice, floxed mice ($Adrb2^{flox/flox}$ or $Gnas^{flox/flox}$ mice) [11,12] were crossed with HSA-Cre(ER^{T2}) mice [13]. Mice used for these matings had been backcrossed onto a C57BL/6 background. To avoid potential developmental changes, Cre recombinase activity was induced in 7–8 week-old HSA-Cre(ER^{T2})-positive homozygous floxed mice by intraperitoneal (i.p.) injection of tamoxifen (2 mg per day dissolved in corn oil) for 5 consecutive days. Tamoxifen-injected Cre-negative homozygous floxed littermates served as control mice.

To generate SKM-specific Gs-DREADD knock-in mice (SKM-GsD mice), heterozygous ROSA26-LSL-Gs-DREADD-CRE-luc mice [14] were crossed with HSA-Cre(ER^{T2}) mice [13]. To induce GsD expression in SKM, Cre-positive hemizygous ROSA26-LSL-Gs-DREADD-CRE-luc mice were injected with tamoxifen as described above. Tamoxifen-injected Cre-negative hemizygous littermates served as control mice in all experiments.

2.3. *In vivo* metabolic studies

All metabolic tests were performed on male littermates (age range 10–30 weeks) using standard protocols. For i.p. glucose tolerance tests (ipGTT), mice were fasted overnight for 15 h and blood glucose levels were measured before (0 min) and at defined time points after i.p. injection of normal saline containing glucose (2 g/kg for mice consuming normal chow; 1 g/kg for mice on HFD). For insulin tolerance tests (ITT), mice were fasted for 4 h and blood glucose levels were measured before (0 min) and at specific time points after i.p. injection of human insulin (0.75 or 1 IU/kg, as indicated; Humulin R, Eli Lilly). Blood glucose levels were determined using a blood glucose meter (Contour; Bayer). To study glucose-stimulated insulin secretion (GSIS), mice were fasted overnight for 15 h, and blood samples were collected in heparinized capillary tubes (Fisher Scientific) before (0 min) and 5, 15, and 30 min following the i.p. injection of glucose (2 or 1 g/kg, as indicated). Samples were centrifuged (5,000 g, 10 min, 4 °C) for plasma collection, and plasma insulin levels were determined using an ultra-sensitive mouse insulin ELISA kit (Crystal Chem, Inc). Where indicated, mice were co-injected or pre-injected i.p. with GPCR agonists (clenbuterol (1 mg/kg) or urocortin 2 (0.1–0.3 mg/kg)) or vehicle for acute treatment experiments.

2.4. Streptozotocin (STZ) model

We used a STZ treatment protocol that destroys about 70–80% of mouse β-cells [15]. Lean WT mice were fasted for 5 h and injected with a relatively low dose (50 mg/kg i.p.) of STZ for 5 consecutive days. Metabolic studies were initiated seven days after the last STZ injection.

2.5. Clozapine-N-Oxide (CNO) administration

To acutely stimulate G_s signaling in SKM, control and SKM-GsD mice received an i.p. injection of CNO (10 mg/kg), either in combination with glucose (ipGTT) or insulin (ITT), respectively.

2.6. *In vivo* [^{14}C]2-deoxyglucose uptake

To measure glucose uptake into individual tissues *in vivo*, mice were fasted overnight for 14–16 h and then injected i.p. with saline containing 2 g/kg glucose and 10 μCi of [^{14}C]2-deoxyglucose ([^{14}C]2-DG) (PerkinElmer). Where indicated, 10 mg/kg CNO was added to acutely stimulate SKM G_s signaling in SKM-GsD mice. Mice were euthanized 2 h later, and SKM and other tissues were harvested. The tissue content of [^{14}C]2-DG-6-phosphate was determined as a measure of SKM glucose uptake, as described previously [16].

2.7. Glycogen measurements

Glycogen content in SKM was determined using a glycogen assay kit (Cayman Chemical) according to the manufacturer's instructions.

2.8. Plasma somatostatin and free fatty acids measurements

Blood samples were collected in EDTA tubes, centrifuged (5,000 g, 10 min, 4 °C) for plasma collection, and somatostatin or free fatty acid levels were determined using a somatostatin EIA kit (Phoenix Pharmaceuticals, Inc.) or the Wako NEFA HR (2) assay (Fujifilm Healthcare Solutions), respectively.

2.9. Static insulin release experiments with isolated mouse islets

Pancreatic islets were isolated from male WT mice (age: ~20 weeks; strain: C57BL/6NTac) by collagenase digestion and Histopaque (Sigma Aldrich, Cat # 1077–1) gradient separation and cultured overnight in RPMI 1640 medium (Thermo Fisher Scientific, Cat # 11,879,020) containing 5.5 mM glucose [17]. On the day of the experiments, islets were preincubated in Krebs–Ringer bicarbonate/HEPES buffer (KRB; 119 mM NaCl, 5 mM KCl, 2.5 mM $CaCl_2$, 1.2 mM $MgCl_2$, 1.2 mM KH_2PO_4, 25 mM $NaHCO_3$, 10 mM HEPES, 0.5% BSA, pH 7.4) containing 3 mM or 16 mM glucose for 30 min. Batches of ten islets were transferred to a 24-well plate (10 islets/well) and incubated in 400 μl of KRB medium with 3 or 16 mM glucose for 1 h at 37 °C, followed by

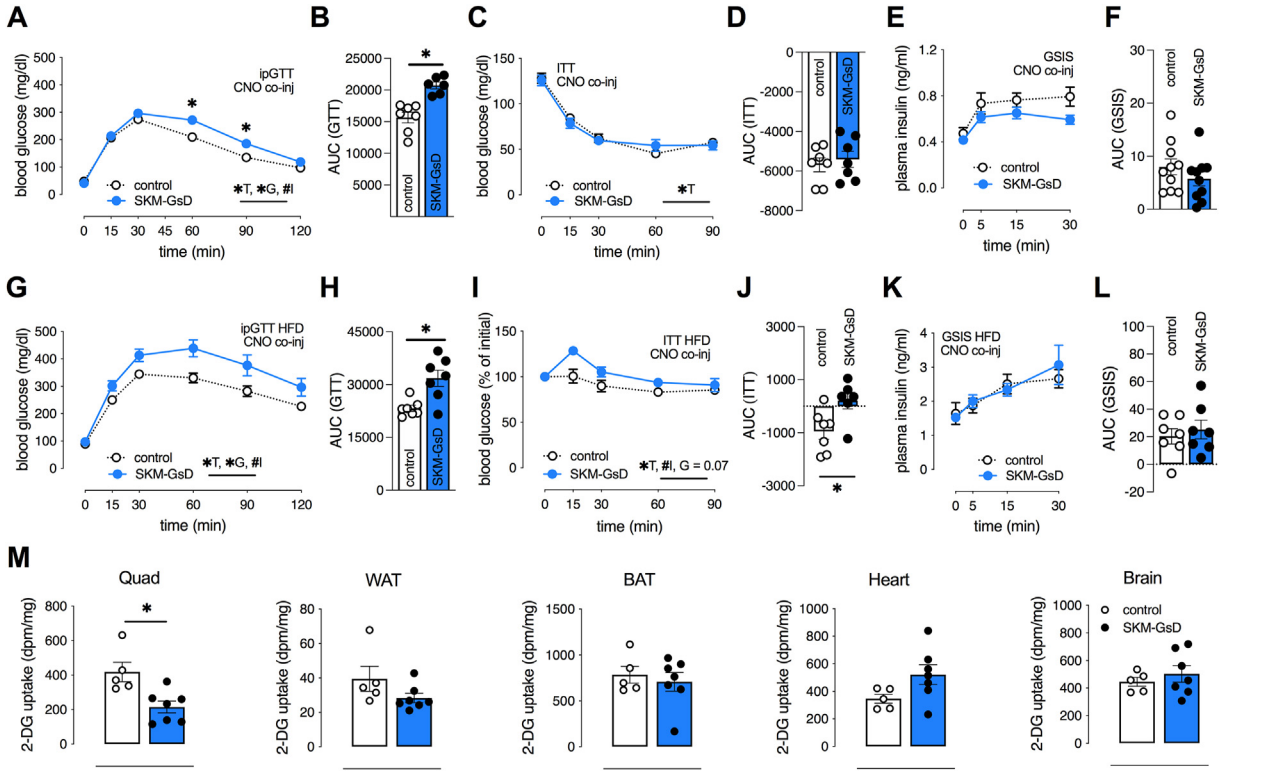

Figure 1: Acute CNO treatment of SKM-Gs-DREADD mice causes impaired glucose tolerance by reducing SKM glucose uptake. (A) Glucose tolerance test (GTT), lean control and SKM-GsD mice (overnight fasted) co-injected i.p. with glucose (2 g/kg) and CNO (10 mg/kg) (n = 6 or 7/group). (B) Area under the curve (AUC) of GTT shown in (A). (C) Insulin tolerance test (ITT), lean control and SKM-GsD mice (fasted for 4 h) co-injected i.p. with insulin (0.75 IU/kg) and CNO (10 mg/kg) (n = 7/group). (D) AUC of ITT shown in (C). (E) Glucose-stimulated insulin secretion (GSIS), lean control and SKM-GsD mice (overnight fasted) co-injected i.p. with glucose (2 g/kg) and CNO (10 mg/kg) (n = 10/group). (F) AUC of GSIS shown in (E). (G) GTT, HFD-induced obese control and SKM-GsD mice (overnight fasted) co-injected i.p. with glucose (1 g/kg) and CNO (10 mg/kg) (n = 7/group). (H) AUC of GTT shown in (G). (I) ITT, HFD-induced obese control and SKM-GsD mice (fasted for 4 h) co-injected i.p. with insulin (0.75 IU/kg) and CNO (10 mg/kg) (n = 6 or 7/group). Data were normalized to initial blood glucose values (251 ± 30 mg/dl vs. 231 ± 20 mg/dl for control and SKM-GsD mice, respectively). (J) AUC of ITT shown in (I). (K) GSIS, HFD-induced obese control and SKM-GsD mice (overnight fasted) co-injected i.p. with glucose (1 g/kg) and CNO (10 mg/kg) (n = 7/group). (L) AUC of GSIS shown in (K). (M) *In vivo* 2-deoxyglucose (2-DG) uptake studies. Lean control and SKM-GsD mice (overnight fasted) were injected with glucose (2 mg/kg i.p.) containing 10 μCi of [^{14}C]2-DG in the presence of CNO (10 mg/kg). Two hours after injections, tissues were collected, and the [^{14}C]2-DG-6-phosphate content was determined in the indicated tissues (n = 5–7/group). Quad, quadriceps muscle; WAT, white adipose tissue; BAT, brown adipose tissue. All studies were carried out on male mice that were at least 8 weeks old. Where indicated mice were fed a HFD for at least eight weeks. Data are presented as means ± SEM. Differences were tested for statistical significance using an unpaired two-tailed Student's t-test (*$p < 0.05$, Figure 1B, D, H, M) or two-way ANOVA (*G, $p < 0.05$ for genotype effect; *T, $p < 0.05$ for time effect; #I, $p < 0.05$ for genotype × time interaction effect; Figure 1A, C, G, I) followed by Sidak's post hoc test (adjusted *$p < 0.05$).

another 1 h incubation step in the presence of test compounds, as indicated. The amount of insulin secreted into the medium during each 1 h incubation period was determined using commercial ELISA kits (Crystal Chem Inc and Mercodia).

2.10. Western blotting experiments

Tissues were isolated quickly, frozen in liquid nitrogen, and stored at −80 °C until use. For western blotting studies, frozen tissues were homogenized in ice-cold RIPA buffer (Sigma Aldrich), and protein concentrations were determined using a BCA protein assay (Thermo Fisher Scientific). Protein extracts were separated on NuPAGE 4–12% Bis-Tris or, for high molecular mass proteins, on 3–8% Tris-Acetate gels (Thermo Fisher Scientific) and blotted onto nitrocellulose membranes (Bio-Rad). Membranes were blocked for 1 h at room temperature in TBS-T (0.1%) containing 5% BSA. Membranes were then incubated overnight with primary antibodies at 4 °C. Following three washing steps with TBS-T (0.1%), membranes were incubated with HRP-conjugated secondary antibodies for 1 h at room temperature. After thorough washing, proteins were visualized with SuperSignal West Dura Extended Duration Substrate (Thermo Fisher Scientific) on the c600 Imaging System (Azure Biosystems). Immunoreactive bands were quantified using Image J Software (NIH).

2.11. Statistics

Data are expressed as mean ± SEM for the indicated number of observations. Data were assessed for statistical significance by 2-way-ANOVA tests, followed by the indicated post hoc tests, or by using a two-tailed unpaired Student's t-test, as appropriate. A p-value of less than 0.05 was considered statistically significant. The specific statistical tests that were used are indicated in the figure legends.

3. RESULTS AND DISCUSSION

3.1. Acute stimulation of a G_s-coupled designer GPCR expressed in SKM decreases glucose uptake into SKM

Since individual GPCRs are widely expressed and systemic administration of agonists *in vivo* usually affects multiple tissues, we took advantage of DREADD technology to clearly define the role of acute SKM G_s stimulation in regulating glucose homeostasis. To explore the *in vivo* metabolic effects caused by acute stimulation of a G_s-linked

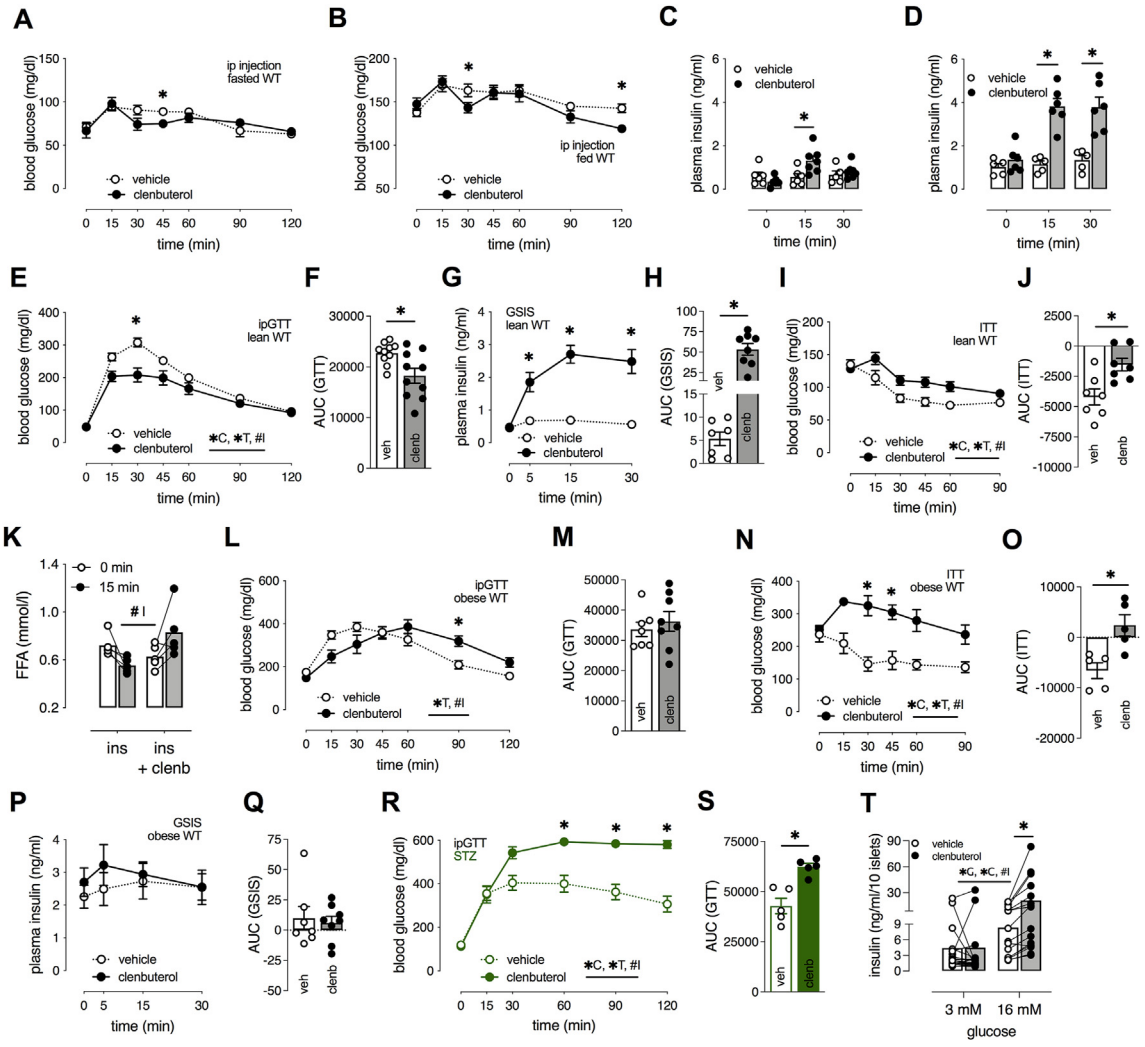

Figure 2: Metabolic effects of acute clenbuterol injection in WT mice. (A) Blood glucose levels in lean WT mice (overnight fasted) following an i.p. injection of clenbuterol (1 mg/kg) or vehicle (n = 10/group). (B) Blood glucose levels in lean, freely fed WT mice following an i.p. injection of clenbuterol (1 mg/kg) or vehicle (n = 8/group). (C) Plasma insulin levels in lean WT mice (overnight fasted) following an i.p. injection of clenbuterol (1 mg/kg) or vehicle (n = 6–7/group). (D) Plasma insulin levels in lean, freely fed WT mice following an i.p. injection of clenbuterol (1 mg/kg) or vehicle (n = 5–6/group). (E) Glucose tolerance test (GTT), lean WT mice (overnight fasted) co-injected i.p. with glucose (2 g/kg) and clenbuterol (1 mg/kg) or vehicle (n = 10/group). (F) Area under the curve (AUC) of GTT shown in (E). (G) Glucose-stimulated insulin secretion (GSIS), lean WT mice (overnight fasted) co-injected i.p. with glucose (2 g/kg) and clenbuterol (1 mg/kg) or vehicle (n = 8/group). (H) AUC of GSIS shown in (G). (I) Insulin tolerance test (ITT), lean WT mice (fasted for 4 h) co-injected i.p. with insulin (0.75 IU/kg) and clenbuterol (1 mg/kg) or vehicle (n = 7/group). (J) AUC of ITT shown in (I). (K) Plasma free fatty acid (FFA) levels following the i.p. co-injection of insulin (ins, 0.75 IU/kg) and clenbuterol (clenb, 1 mg/kg) or vehicle (n = 5/group). (L) GTT, HFD-induced obese WT mice (overnight fasted) co-injected i.p. with glucose (1 g/kg) and clenbuterol (1 mg/kg) or vehicle (n = 7 or 8/group). (M) AUC of GTT shown in (L). (N) ITT, HFD-induced obese WT mice (fasted for 4 h) co-injected i.p. with insulin (0.75 IU/kg) and clenbuterol (1 mg/kg) or vehicle (n = 5 or 6/group). (O) AUC of ITT shown in (N). (P) GSIS, HFD-induced obese WT mice (overnight fasted) co-injected i.p. with glucose (1 g/kg) and clenbuterol (1 mg/kg) or vehicle (n = 7 or 8/group). (Q) AUC of GSIS shown in (P). (R) GTT, streptozotocin (STZ)-induced diabetic WT mice (overnight fasted) co-injected i.p. with glucose (1 g/kg) and clenbuterol (1 mg/kg) or vehicle (n = 5/group). (S) AUC of GTT shown in (R). (T) Static islet incubation assay, pancreatic islets isolated from lean WT mice were incubated for 1 h in Krebs–Ringer buffer containing 3 mM or 16 mM glucose, followed by the addition of clenbuterol (1 μM) for another 1 h, as indicated. Medium was collected for insulin measurements (n = 16 or 19 islet preparations/group from 4 or 5 mice). All studies were carried out with male mice that were at least ten weeks old. Where indicated mice were fed a HFD for at least eight weeks. Data presented as means ± SEM. Differences were tested for statistical significance using an unpaired two-tailed Student's t-test (*p < 0.05, Figure 2A–D, F–H, J, O, S) or two-way ANOVA (*C, p < 0.05 for clenbuterol effect; *T, p < 0.05 for time effect; *G, p < 0.05 for glucose effect; #I, p < 0.05 for clenbuterol x time/glucose interaction effect; Figure 2E, I, K, L, N, R, T) followed by Sidak's post hoc test (*adjusted p < 0.05).

GPCR in SKM, we generated mice that expressed a G_s-coupled DREADD (GsD) [18] under the transcriptional control of the SKM-specific human α-skeletal actin (HSA) promoter (SKM-GsD mice). Control and SKM-GsD mice did not show any metabolic differences in the absence of CNO (Meister et al. Nature Communications, in press). Following CNO (10 mg/kg i.p.) treatment, SKM-GsD mice maintained on regular chow or a HFD displayed a significant impairment in glucose tolerance (Figure 1A, B, G, H). In contrast to lean SKM-GsD mice (Figure 1C, D), HFD SKM-GsD mice displayed a slight deficit in insulin tolerance (Figure 1I, J) as compared to their control littermates. Acute administration of CNO to SKM-GsD and control mice had no significant effect on glucose-stimulated insulin secretion (GSIS, Figure 1E, F, K, L). To investigate whether glucose uptake by SKM was altered in CNO-treated SKM-GsD mice, we co-injected (i.p.) SKM-GsD and control mice with CNO (10 mg/kg) and glucose (2 g/kg) containing 10 μCi of [^{14}C]-2-deoxyglucose ([^{14}C]-2-DG). Accumulation of the [^{14}C]-2-DG

metabolite, [^{14}C]-2-DG-6-phosphate, was determined as a measure of glucose uptake. We found that CNO-treated SKM-GsD mice showed reduced glucose uptake into SKM (quadriceps muscle), as compared to CNO-injected control littermates (Figure 1M). Glucose uptake into adipose tissues, heart, and brain remained unaffected following CNO injection of SKM-GsD mice (Figure 1M). Taken together, these data strongly suggest that acute stimulation of SKM G_s signaling impairs blood glucose uptake into SKM. In contrast, we previously demonstrated that chronic activation of SKM G_s signaling leads to improved glucose tolerance without affecting insulin sensitivity or secretion (Meister et al. Nature Communications, in press).

We next mined RNA-Seq data to identify GPCRs expressed by mouse quadriceps muscle. This analysis showed that the β_2-adrenergic receptor (β_2-AR) and the corticotropin-releasing hormone receptor 2 (CRF_2), two G_s-coupled receptors, were highly expressed in SKM (Supplemental Fig. 1). These receptors are also expressed in other metabolically relevant tissues, although at lower levels [9]. Previous studies have led to contradictory results regarding the roles of these receptors in regulating glucose homeostasis [19–25].

3.2. Acute β_2-AR activation improves glucose tolerance only in healthy lean mice

To study the acute *in vivo* metabolic effects of β_2-AR stimulation, we initially administered clenbuterol, a β_2-AR-selective agonist, to lean wild type (WT) mice. After a single clenbuterol injection (1 mg/kg i.p.), lean WT mice (either freely fed or fasted for 15 h) showed only slight differences in blood glucose excursions after a single clenbuterol injection (1 mg/kg i.p.), as compared to control mice injected with vehicle alone (Figure 2A, B). The clenbuterol bolus caused a significant increase in plasma insulin levels (Figure 2C, D). During a glucose tolerance test (GTT), lean WT mice co-injected i.p. with glucose (2 g/kg) and clenbuterol showed significantly reduced blood glucose levels, as compared to control mice injected with glucose alone (Figure 2E, F). Acute clenbuterol injection led to a dramatic increase in GSIS in lean WT mice (Figure 2G, H). An insulin tolerance test (ITT) demonstrated that co-injection of insulin (0.75 IU/kg i.p.) with clenbuterol decreased insulin sensitivity (Figure 2I, J). Furthermore, clenbuterol injection during the ITT caused an increase in plasma free fatty acid (FFA) levels (Figure 2K), probably due to the activation of β_2-ARs expressed by adipose tissue [26].

We tested whether acute clenbuterol administration was able to improve glucose homeostasis in a model of diet-induced obesity. WT mice that were fed a high fat diet (HFD) for at least 8 weeks were characterized in several metabolic tests, either in the absence or presence of co-injected clenbuterol. When obese HFD mice were subjected to a GTT, i.p. co-injection of glucose (1 g/kg) and clenbuterol had no clear effect on glucose tolerance (Figure 2L, M). As observed with lean WT mice, acute clenbuterol injection of obese WT mice led to a severe decrease in insulin tolerance (Figure 2N, O). In contrast to the outcome of GSIS studies with lean WT mice (Figure 2G, H), acute clenbuterol treatment did not potentiate GSIS in obese WT mice (Figure 2P, Q).

To mimic the loss of β-cell mass characteristic for advanced T2D, we used a streptozotocin (STZ) treatment protocol known to destroy about 70–80% of mouse β-cells [15]. When STZ-treated mice were co-injected i.p. with glucose (1 g/kg) and clenbuterol, they displayed even more pronounced glucose intolerance than STZ-treated mice treated with glucose alone (Figure 2R, S). This phenotype is opposite to the one observed with lean healthy mice (Figure 2E, F), mimicking the effects of SKM-GsD stimulation *in vivo* (Figure 1A, B). These results strongly suggest that the clenbuterol-induced improvements in glucose tolerance observed in lean healthy mice (Figure 2E, F) are primarily driven by enhanced insulin release (Figure 2G, H). To test the ability of clenbuterol to directly stimulate pancreatic insulin secretion, we incubated isolated WT mouse islets in low (3 mM) and high glucose (16 mM) medium in the presence or absence of clenbuterol (1 μM). Clenbuterol treatment significantly enhanced GSIS (Figure 2T), indicating that activation of islet β_2-ARs promotes insulin secretion [27,28]. Because of the high expression of the β_2-AR in SKM and the striking phenotypes displayed by the SKM-GsD mice, we next explored the potential contribution of SKM β_2-ARs to the acute *in vivo* metabolic effects of clenbuterol. To address this question, we used mice that lacked β_2-ARs selectively in SKM (SKM-β_2-AR-KO mice).

Acute clenbuterol injection retained the ability to trigger improved glucose tolerance in SKM-β_2-AR-KO (Figure 3A, B), consistent with the concept that this beneficial metabolic effect was mainly driven by increased insulin release (Figure 2G, H, T). However, we observed a slight reversal of the clenbuterol-mediated impairment in insulin sensitivity in SKM-β_2-AR-KO (Figure 3C, D), suggesting that the clenbuterol effect during the ITT is at least partially dependent on the activation of SKM β_2-ARs.

To explore the potential roles of SKM β_2-ARs in regulating the responsiveness of SKM to insulin, we co-injected lean WT mice with insulin in the presence or absence of clenbuterol and isolated quadriceps muscles 15 min later. While clenbuterol had no significant effect on insulin-induced AKT or GSK3β phosphorylation (Supplemental Figs. 2A and B), co-injection of insulin with clenbuterol led to a significant increase in the inhibitory phosphorylation of glycogen synthase at S641 in WT mice (Figure 3E, F). In agreement with this observation, glycogen levels were significantly decreased in SKM of WT mice that were co-injected with insulin and clenbuterol, as compared to mice injected with insulin alone (Figure 3G). This clenbuterol effect was not observed in SKM derived from SKM-β_2-AR-KO mice, indicating that the clenbuterol-induced decrease in SKM glycogen levels is mediated by SKM β_2-ARs (Figure 3H).

Our data strongly suggest that acute injection of clenbuterol improves glucose tolerance primarily by increasing plasma insulin levels through direct stimulation of islet β_2-ARs (Figure 2C–H, T). In agreement with this observation, it has been reported that activation of β_2-ARs expressed by mouse or human pancreatic β-cells promotes insulin secretion [27,28]. In contrast to a previous proposal [25], acute SKM β_2-AR signaling did not contribute to this beneficial metabolic effect, since acute clenbuterol injection retained the ability to improve glucose tolerance in mice lacking β_2-ARs in SKM (Figure 3A, B). These new data clearly demonstrate the importance of using cell type-specific mutant mouse models in clarifying the physiological roles of widely expressed GPCRs like the β_2-AR.

Acute clenbuterol injection failed to improve whole-body glucose homeostasis in obese mice consuming a HFD (Figure 2L, M) or after STZ-induced loss of β-cells (Figure 2R, S). The most likely explanation for these findings is that the clenbuterol-induced decrease in insulin tolerance (Figure 2I, J, N, O) is due to elevated plasma FFA levels caused by enhanced lipolysis (Figure 2K). We have recently shown that selective activation of G_s-coupled receptors in adipose tissue induces lipolysis [29]. It is likely that clenbuterol-stimulated glycogen breakdown in SKM also contributes to impaired insulin tolerance (Figure 3E, G). Increased glycogenolysis is predicted to slow down glucose influx into SKM [30]. The negative metabolic effect of acute stimulation of SKM β_2-ARs on whole-body glucose homeostasis becomes evident in the mouse model of HFD-induced insulin resistance and STZ-induced β-cell loss, where acute clenbuterol was unable to increase insulin

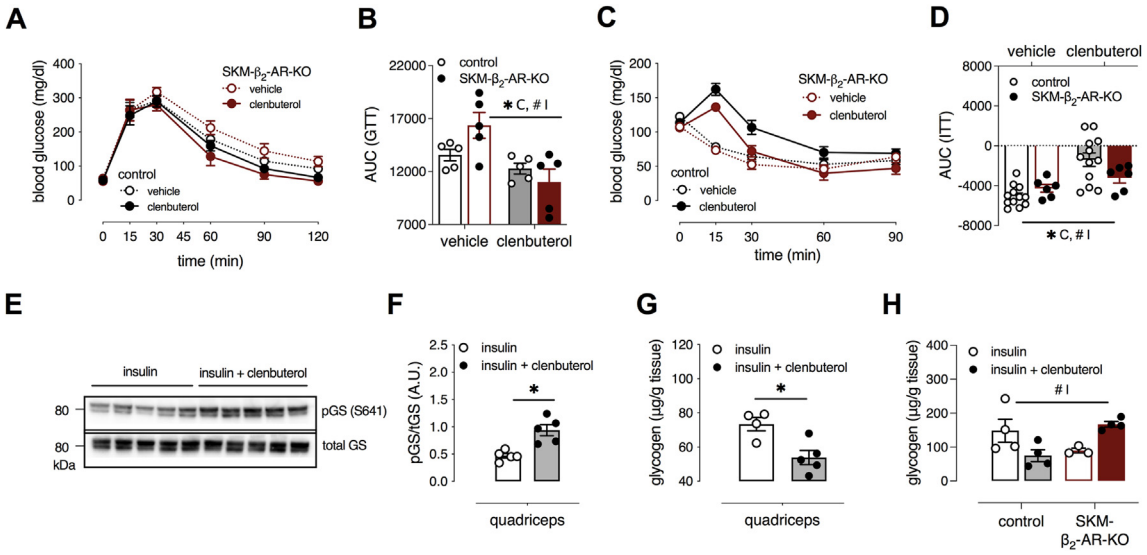

Figure 3: SKM β_2-AR-mediated metabolic effects of acute clenbuterol injection. (A) Glucose tolerance test (GTT), lean control and SKM-β_2-AR-KO mice (overnight fasted) co-injected i.p. with glucose (2 g/kg) and clenbuterol (1 mg/kg) or vehicle (n = 5/group). (B) Area under the curve (AUC) of GTT shown in (A). (C) Insulin tolerance test (ITT, 0.75 IU/kg insulin) performed with 4 h-fasted control and SKM-β_2-AR-KO mice (n = 6 or 12/group). (D) AUC of ITT shown in (C). (E–G) Drug effects on SKM glycogen synthase (GS) phosphorylation (pGS) and SKM glycogen levels. Lean WT mice were fasted for 4 h and then co-injected i.p. with insulin (0.75 IU/kg) and clenbuterol (1 mg/kg) or vehicle. SKM tissues (quadriceps muscle) were isolated 15 min post-injection (n = 4 or 5/group), followed by the determination of pGS and total GS protein levels (E, F) and SKM glycogen content (G). (H) Glycogen levels in SKM (quadriceps muscle) of lean control and SKM-β_2-AR-KO mice 15 min after i.p. co-injection of insulin (0.75 IU/kg) and clenbuterol (1 mg/kg) or vehicle (n = 3 or 4/group). All studies were carried out with male mice that were at least ten weeks old. Data presented as means ± SEM. Differences were tested for statistical significance using an unpaired two-tailed Student's t-test (*$p < 0.05$) or two-way ANOVA (*C, $p < 0.05$ for clenbuterol effect, #I, $p < 0.05$ for clenbuterol × genotype interaction effect).

secretion (obese mice; Figure 2P) or caused further impaired glucose tolerance (STZ-treated mice; Figure 2R, S).

It is well known that activation of the sympathetic nervous system promotes glycogen breakdown in SKM cells via activation of G_s-coupled β_2-ARs [31]. The resulting increase in intracellular glucose levels is most probably the cause of the impaired SKM glucose uptake observed after acute GsD stimulation in SKM cells. In comparison, chronic stimulation of SKM G_s signaling by clenbuterol led to a significant increase in glucose uptake, most likely resulting from metabolic reprogramming of SKM cells causing enhanced glucose utilization (Meister et al. Nature Communications, in press).

3.3. Acute CRF_2 activation increases blood glucose levels

As mentioned earlier, the G_s-coupled CRF_2 receptor is enriched in SKM tissue (Supplemental Fig. 1). An acute bolus of urocortin 2 (UCN2; 0.1 mg/kg i.p.), a selective CRF_2 agonist [32], increased blood glucose levels in overnight fasted and *ad libitum* fed lean WT mice (Figure 4A, B, E, F). UCN2 injection reduced basal plasma insulin levels in these mice (Figure 4C, D, G, H). Co-injection of glucose (2 g/kg) with UCN2 resulted in impaired glucose tolerance (Figure 4I, J) and reduced GSIS (Figure 4K).

In vitro studies with isolated pancreatic islets have shown that stimulation of CRF_2 receptors causes an increase in somatostatin release [33]. We did not observe differences in plasma somatostatin levels following the co-administration of glucose and UCN2, as compared to glucose alone (Supplemental Fig. 3A). Surprisingly, UCN2 (100 nM) did not affect insulin release in isolated pancreatic islets derived from WT mice during static incubation assays (Supplemental Fig. 3B). Plasma FFA levels also remained unaffected by the UCN2 bolus (Supplemental Fig. 3C), and UCN2 injection did not affect insulin sensitivity in lean WT mice (Figure 4M, N).

UCN2 decreased glucose tolerance in HFD-induced obese mice (Figure 4O, P). In contrast to lean mice, UCN2 reduced insulin sensitivity in a time-dependent manner in obese mice (Figures 4Q, R and Supplemental Fig. 3D). The effect was most prominent when UCN2 was administered 15 min prior to the insulin bolus (Figure 4S, T).

Previous data obtained with cultured myocytes suggest that acute treatment with UCN2 reduces insulin signaling in SKM [34]. Further, *ex vivo* experiments have shown that UCN2 dose-dependently increases cAMP in mouse SKM [35]. To test the hypothesis that some of the observed metabolic effects of UCN2 involved SKM CRF_2 receptors and stimulation of SKM G_s signaling, we studied mice that lack G_s ($G\alpha_s$) selectively in SKM (SKM-Gs-KO mice). We subjected these mice to several metabolic tests in the presence or absence of UCN2. The increases in blood glucose levels following UCN2 injection alone and in combination with glucose or insulin were not dependent on SKM G_s signaling, since SKM-Gs-KO mice showed similar metabolic phenotypes as their control littermates (Supplemental Figs. 4A–F).

Previous studies examining the role of SKM CRF_2 receptors in metabolic disorders have yielded conflicting results. Both increase [36] and decrease [19] in UCN2-stimulated SKM glucose uptake have been described using *in vitro* cell systems. UCN2- and CRF_2-KO mice show improvements in whole-body glucose homeostasis [34,37], but mice overexpressing UCN2 showed the same phenotype [20,36]. Our study clearly demonstrates that acute UCN2 injection *in vivo* impairs glucose homeostasis by decreasing insulin secretion (Figure 4A–K).

CRF_2 receptors are highly expressed in pancreatic δ-cells [33], and previous *in vitro* studies suggest that UCN3, another CRF_2 receptor agonist, can modulate somatostatin and glucagon secretion from pancreatic islets [33,38]. In this study, we did not observe an increase in plasma somatostatin levels following co-injection of glucose and UCN2 (Supplemental Fig. 3A), and UCN2 (100 nM) had no effect on

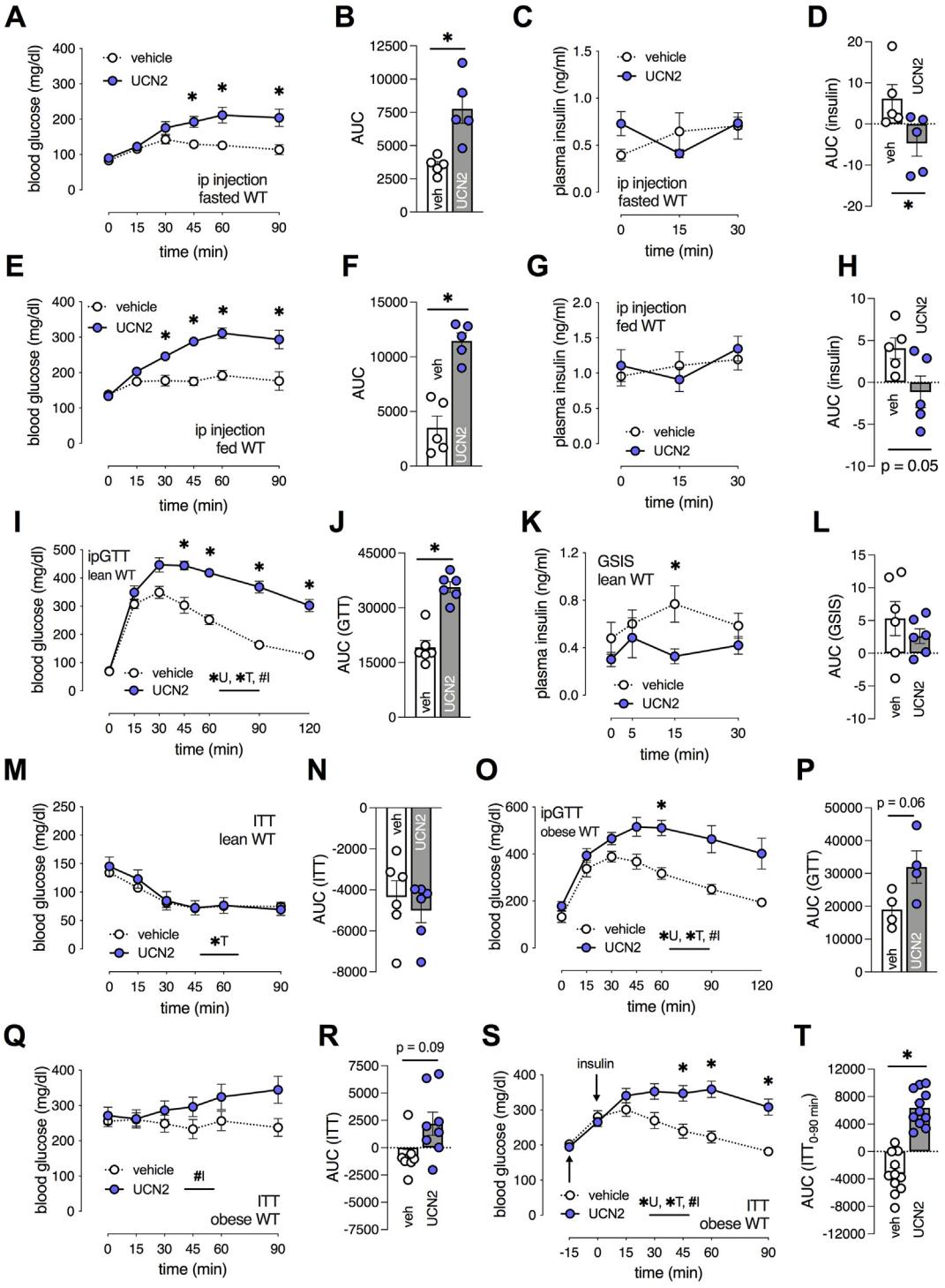

Figure 4: Metabolic effects of acute urocortin 2 injection. (A) Blood glucose levels in lean WT mice (overnight fasted) following an i.p. injection of urocortin 2 (UCN2, 0.1 mg/kg) or vehicle (n = 5/group). (B) Area under the curve (AUC) of (A). (C) Plasma insulin levels in lean WT mice (overnight fasted) following an i.p. injection of UCN2 (0.1 mg/kg) or vehicle (n = 5/group). (D) Area under the curve (AUC) of (C). (E) Blood glucose levels in lean, freely fed WT mice following an i.p. injection of UCN2 (0.1 mg/kg) or vehicle (n = 5/group). (F) AUC of (E). (G) Plasma insulin levels in lean, freely fed WT mice following an i.p. injection of UCN2 (0.1 mg/kg) or vehicle (n = 5/group). (H) AUC of (G). (I) Glucose tolerance test (GTT), lean WT mice (overnight fasted) co-injected i.p. with glucose (2 g/kg) and UCN2 (0.1 mg/kg) or vehicle (n = 6/group). (J) AUC of GTT shown in (I). (K) Glucose-stimulated insulin secretion (GSIS), lean WT mice (overnight fasted) co-injected i.p. with glucose (2 g/kg) and UCN2 (0.1 mg/kg) or vehicle (n = 6/group). (L) AUC of GSIS shown in (K). (M) Insulin tolerance test (ITT), lean WT mice (fasted for 4 h) co-injected i.p. with insulin (0.75 IU/kg) and UCN2 (0.1 mg/kg) or vehicle (n = 6/group). (N) AUC of ITT shown in (M). (O) GTT, HFD-induced obese WT mice (overnight fasted) co-injected i.p. with glucose (1 g/kg) and UCN2 (0.1 mg/kg) or vehicle (n = 4/group). (P) AUC of GTT shown in (O). (Q) ITT, HFD-induced obese WT mice (fasted for 4 h) co-injected i.p. with insulin (0.75 IU/kg) and UCN2 (0.3 mg/kg) or vehicle (n = 5 or 6/group). (R) AUC of ITT shown in (Q). (S) ITT, HFD-induced obese WT mice (fasted for 4 h) pre-injected i.p. with UCN2 (0.3 mg/kg) or vehicle, followed by an insulin bolus (0.75 IU/kg) (n = 11/group). (T) AUC of ITT shown in (S). All studies were carried out on male mice that were at least 8 weeks old. Where indicated, mice were fed a HFD for at least eight weeks. Data presented as means ± SEM. Differences were tested for statistical significance using an unpaired two-tailed Student's t-test (*$p < 0.05$, Figure 4A, B, D, E, F, H, J, K, P, R, T) or two-way ANOVA (*U, $p < 0.05$ for UCN2 effect; *T, $p < 0.05$ for time effect; #I, $p < 0.05$ for UCN2 x time interaction effect; Figure 4I, M, O, Q, S) followed by Sidak's post hoc test (*adjusted $p < 0.05$).

insulin release from isolated WT pancreatic islets (Supplemental Fig. 3B). One likely explanation for the discrepancy between the *in vivo* insulin data (Figure 4C,D, G, H, K) and the outcome of the *in vitro* studies with isolated islets (Supplemental Fig. 3B) is that specific circulating factors or neuronal inputs that contribute to UCN2-mediated insulin release *in vivo* are absent in the islet incubation assay.

Studies with SKM-Gs-KO mice showed that the metabolic effects of acute UCN2 administration are not dependent on SKM G_s signaling (Supplemental Fig. 4). Further studies with conditional KO mice are necessary to determine whether the metabolic improvements seen after long-term treatment with UCN2 peptides [39] or UCN2 gene transfer [36] are indeed mediated by SKM CRF_2 receptors.

Using a chemogenetic approach we showed that acute activation of SKM G_s signaling decreased glucose uptake into SKM *in vivo*, leading to significant impairments in whole-body glucose homeostasis. However, the acute *in vivo* stimulation of two SKM-enriched G_s-coupled receptors (β_2-AR and CRF_2) resulted in metabolic effects that were mostly SKM-independent and predominantly mediated by altered insulin levels, probably due to altered insulin secretion from pancreatic islets.

Our study further highlights the need to distinguish between acute and long-term effects of GPCR agonists. Different drug exposure times *in vivo* can result in different tissue-specific effects, and *in vitro* and *ex vivo* data need to be carefully validated in whole-body settings in order to draw conclusions about the ultimate metabolic outcome. Our data provide an excellent example for the concept that acute administration of GPCR agonists needs to be complemented by chronic agonist treatment studies to properly assess translationally relevant metabolic outcomes.

In the present study, we demonstrated that acute activation of SKM G_s signaling caused an impairment in glucose tolerance. In contrast, a recent study (Meister et al. Nature Communications, in press) demonstrated that chronic activation of SKM G_s signaling leads to improved whole-body glucose homeostasis in both lean and obese mice. This latter finding raises the possibility that drugs able to selectively stimulate SKM G_s signaling may prove to be useful as novel antidiabetic drugs.

ACKNOWLEDGEMENTS

This research was funded by the Intramural Research Program of the National Institute of Diabetes and Digestive and Kidney Diseases (NIDDK, NIH). We thank Dr. Daniel Metzger (Université de Strasbourg, Illkirch, France) for providing the HSA-Cre(ERT2) mice, Dr. Rebecca Berdeaux (Houston Medical School, Houston, USA) for providing the ROSA26-LSL-Gs-DREADD-CRE-luc mice, and Dr. Gerard Karsenty for providing the floxed Adrb2 mice (Columbia University, New York, USA). We thank Dr. Erik A. Richter (University of Copenhagen, Denmark) for his advice and valuable discussions on skeletal muscle physiology. We further thank Yinghong Cui (NIDDK) for mouse colony management and Yinyan Ma (NIDDK) for technical assistance with the 2-DG uptake experiments.

AUTHOR CONTRIBUTIONS

J.M., D.B.J.B. and J.W. conceived and designed the study. J.M., D.B.J.B., L.F.B., R.L. and O.G. performed the experiments. L.L. designed and performed the static islet experiments. J.M., D.B.J.B., J.R.K., L.L., R.L. and O.G. analyzed and interpreted the experimental data. M.C. and L.S.W. provided mutant mouse models and helpful advice. J.R.K, M.K. and T.E.J. supervised part of the studies and provided critical guidance regarding the preparation of the manuscript. J.M., D.B.J.B and J.W. wrote and revised the manuscript. J.M. prepared the first draft. All authors approved the final version of the manuscript.

CONFLICT OF INTEREST

The authors have declared that no conflict of interest exists.

APPENDIX A. SUPPLEMENTARY DATA

Supplementary data to this article can be found online at https://doi.org/10.1016/j.molmet.2021.101415.

REFERENCES

1 Meister, J., Wang, L., Pydi, S.P., Wess, J., 2021. Chemogenetic approaches to identify metabolically important GPCR signaling pathways: therapeutic implications. Journal of Neurochemistry. https://doi.org/10.1111/jnc.15314.

2 Armbruster, B.N., Li, X., Pausch, M.H., Herlitze, S., Roth, B.L., 2007. Evolving the lock to fit the key to create a family of G protein-coupled receptors potently activated by an inert ligand. Proceedings of the National Academy of Sciences of the U S A 104(12):5163—5168. https://doi.org/10.1073/pnas.0700293104.

3 Roth, B.L., 2016. DREADDs for neuroscientists. Neuron 89(4):683—694. https://doi.org/10.1016/j.neuron.2016.01.040.

4 Hu, J., Stern, M., Gimenez, L.E., Wanka, L., Zhu, L., Rossi, M., et al., 2016. Protein-biased designer G protein-coupled receptor useful for studying the physiological relevance of Gq/11-dependent signaling pathways. Journal of Biological Chemistry 291(15):7809—7820. https://doi.org/10.1074/jbc.M115.702282.

5 Nagai, Y., Miyakawa, N., Takuwa, H., Hori, Y., Oyama, K., Ji, B., et al., 2020. Deschloroclozapine, a potent and selective chemogenetic actuator enables rapid neuronal and behavioral modulations in mice and monkeys. Nature Neuroscience 23(9):1157—1167. https://doi.org/10.1038/s41593-020-0661-3.

6 Thompson, K.J., Khajehali, E., Bradley, S.J., Navarrete, J.S., Huang, X.P., Slocum, S., et al., 2018. DREADD agonist 21 is an effective agonist for muscarinic-based DREADDs in vitro and in vivo. ACS Pharmacol Transl Sci 1(1):61—72. https://doi.org/10.1021/acsptsci.8b00012.

7 Wang, L., Zhu, L., Meister, J., Bone, D.B.J., Pydi, S.P., Rossi, M., et al., 2021. Use of DREADD technology to identify novel targets for antidiabetic drugs. Annual Review of Pharmacology and Toxicology 61:421—440. https://doi.org/10.1146/annurev-pharmtox-030220-121042.

8 DeFronzo, R.A., Tripathy, D., 2009. Skeletal muscle insulin resistance is the primary defect in type 2 diabetes. Diabetes Care 32(Suppl 2):S157—S163. https://doi.org/10.2337/dc09-S302.

9 Regard, J.B., Sato, I.T., Coughlin, S.R., 2008. Anatomical profiling of G protein-coupled receptor expression. Cell 135(3):561—571. https://doi.org/10.1016/j.cell.2008.08.040.

10 Bone, D.B.J., Meister, J., Knudsen, J.R., Dattaroy, D., Cohen, A., Lee, R., et al., 2019. Skeletal muscle-specific activation of Gq signaling maintains glucose homeostasis. Diabetes 68(6):1341—1352. https://doi.org/10.2337/db18-0796.

11 Shi, Y., Yadav, V.K., Suda, N., Liu, X.S., Guo, X.E., Myers Jr., M.G., et al., 2008. Dissociation of the neuronal regulation of bone mass and energy metabolism by leptin in vivo. Proceedings of the National Academy of Sciences of the U S A 105(51):20529—20533. https://doi.org/10.1073/pnas.0808701106.

12 Chen, M., Feng, H.Z., Gupta, D., Kelleher, J., Dickerson, K.E., Wang, J., et al., 2009. G(s)alpha deficiency in skeletal muscle leads to reduced muscle mass, fiber-type switching, and glucose intolerance without insulin resistance or deficiency. American Journal of Physiology - Cell Physiology 296(4):C930—C940. https://doi.org/10.1152/ajpcell.00443.2008.

13 Schuler, M., Ali, F., Metzger, E., Chambon, P., Metzger, D., 2005. Temporally controlled targeted somatic mutagenesis in skeletal muscles of the mouse. Genesis (New York, N.Y. 2000) 41(4):165—170. https://doi.org/10.1002/gene.20107.

14 Akhmedov, D., Mendoza-Rodriguez, M.G., Rajendran, K., Rossi, M., Wess, J., Berdeaux, R., 2017. Gs-DREADD knock-in mice for tissue-specific, temporal stimulation of cyclic AMP signaling. Molecular and Cellular Biology 37(9). https://doi.org/10.1128/mcb.00584-16.

15 Jain, S., Ruiz de Azua, I., Lu, H., White, M.F., Guettier, J.M., Wess, J., 2013. Chronic activation of a designer G(q)-coupled receptor improves beta cell function. Journal of Clinical Investigation 123(4):1750–1762. https://doi.org/10.1172/jci66432.

16 Li, Y.Q., Shrestha, Y.B., Chen, M., Chanturiya, T., Gavrilova, O., Weinstein, L.S., 2016. Gsalpha deficiency in adipose tissue improves glucose metabolism and insulin sensitivity without an effect on body weight. Proceedings of the National Academy of Sciences of the U S A 113(2):446–451. https://doi.org/10.1073/pnas.1517142113.

17 Barella, L.F., Rossi, M., Pydi, S.P., Meister, J., Jain, S., Cui, Y., et al., 2021. β-Arrestin-1 is required for adaptive β-cell mass expansion during obesity. Nature Communications 12(1):3385. https://doi.org/10.1038/s41467-021-23656-1.

18 Guettier, J.M., Gautam, D., Scarselli, M., de Azua, I.R., Li, J.H., Rosemond, E., et al., 2009. A chemical-genetic approach to study G protein regulation of beta cell function in vivo. Proceedings of the National Academy of Sciences of the U S A 106(45):19197–19202. https://doi.org/10.1073/pnas.0906593106.

19 Chao, H., Li, H., Grande, R., Lira, V., Yan, Z., Harris, T.E., et al., 2015. Involvement of mTOR in type 2 CRF receptor inhibition of insulin signaling in muscle cells. Molecular Endocrinology 29(6):831–841. https://doi.org/10.1210/me.2014-1245.

20 Gao, M.H., Giamouridis, D., Lai, N.C., Guo, T., Xia, B., Kim, Y.C., et al., 2020. Urocortin 2 gene transfer improves glycemic control and reduces retinopathy and mortality in murine insulin deficiency. Molecular Theraphy Methods Clinical Dev 17:220–233. https://doi.org/10.1016/j.omtm.2019.12.002.

21 Jensen, J., Aslesen, R., Ivy, J.L., Brors, O., 1997. Role of glycogen concentration and epinephrine on glucose uptake in rat epitrochlearis muscle. American Journal of Physiology 272(4 Pt 1):E649–E655. https://doi.org/10.1152/ajpendo.1997.272.4.E649.

22 Kalinovich, A., Dehvari, N., Aslund, A., van Beek, S., Halleskog, C., Olsen, J., et al., 2020. Treatment with a beta-2-adrenoceptor agonist stimulates glucose uptake in skeletal muscle and improves glucose homeostasis, insulin resistance and hepatic steatosis in mice with diet-induced obesity. Diabetologia 63(8):1603–1615. https://doi.org/10.1007/s00125-020-05171-y.

23 Ngala, R.A., O'Dowd, J., Wang, S.J., Agarwal, A., Stocker, C., Cawthorne, M.A., et al., 2008. Metabolic responses to BRL37344 and clenbuterol in soleus muscle and C2C12 cells via different atypical pharmacologies and beta2-adrenoceptor mechanisms. British Journal of Pharmacology 155(3):395–406. https://doi.org/10.1038/bjp.2008.244.

24 Ngala, R.A., O'Dowd, J., Wang, S.J., Stocker, C., Cawthorne, M.A., Arch, J.R., 2009. Beta2-adrenoceptors and non-beta-adrenoceptors mediate effects of BRL37344 and clenbuterol on glucose uptake in soleus muscle: studies using knockout mice. British Journal of Pharmacology 158(7):1676–1682. https://doi.org/10.1111/j.1476-5381.2009.00472.x.

25 Sato, M., Dehvari, N., Oberg, A.I., Dallner, O.S., Sandström, A.L., Olsen, J.M., et al., 2014. Improving type 2 diabetes through a distinct adrenergic signaling pathway involving mTORC2 that mediates glucose uptake in skeletal muscle. Diabetes 63(12):4115–4129. https://doi.org/10.2337/db13-1860.

26 Kim, H.K., Della-Fera, M.A., Hausman, D.B., Baile, C.A., 2010. Effect of clenbuterol on apoptosis, adipogenesis, and lipolysis in adipocytes. Journal of Physiology & Biochemistry 66(3):197–203. https://doi.org/10.1007/s13105-010-0024-8.

27 Santulli, G., Lombardi, A., Sorriento, D., Anastasio, A., Del Giudice, C., Formissano, P., et al., 2012. Age-related impairment in insulin release: the essential role of β(2)-adrenergic receptor. Diabetes 61(3):692–701. https://doi.org/10.2337/db11-1027.

28 Lacey, R.J., Berrow, N.S., London, N.J., Lake, S.P., James, R.F., Scarpello, J.H., et al., 1990. Differential effects of beta-adrenergic agonists on insulin secretion from pancreatic islets isolated from rat and man. Journal of Molecular Endocrinology 5(1):49–54. https://doi.org/10.1677/jme.0.0050049.

29 Wang, L., Pydi, S.P., Cui, Y., Zhu, L., Meister, J., Gavrilova, O., et al., 2019. Selective activation of Gs signaling in adipocytes causes striking metabolic improvements in mice. Molecular Metabolism 27:83–91. https://doi.org/10.1016/j.molmet.2019.06.018.

30 Sylow, L., Kleinert, M., Richter, E.A., Jensen, T.E., 2016. Exercise-stimulated glucose uptake - regulation and implications for glycaemic control. Nature Reviews Endocrinology. https://doi.org/10.1038/nrendo.2016.162.

31 Roatta, S., Farina, D., 2010. Sympathetic actions on the skeletal muscle. Exercise and Sport Sciences Reviews 38(1):31–35. https://doi.org/10.1097/JES.0b013e3181c5cde7.

32 Squillacioti, C., Pelagalli, A., Liguori, G., Mirabella, N., 2019. Urocortins in the mammalian endocrine system. Acta Veterinaria Scandinavica 61(1):46. https://doi.org/10.1186/s13028-019-0480-2.

33 van der Meulen, T., Donaldson, C.J., Cáceres, E., Hunter, A.E., Cowing-Zitron, C., Pound, L.D., et al., 2015. Urocortin3 mediates somatostatin-dependent negative feedback control of insulin secretion. Nature Medicine 21(7):769–776. https://doi.org/10.1038/nm.3872.

34 Chen, A., Brar, B., Choi, C.S., Rousso, D., Vaughan, J., Kuperman, Y., et al., 2006. Urocortin 2 modulates glucose utilization and insulin sensitivity in skeletal muscle. Proceedings of the National Academy of Sciences of the U S A 103(44):16580–16585. https://doi.org/10.1073/pnas.0607337103.

35 Hinkle, R.T., Donnelly, E., Cody, D.B., Bauer, M.B., Isfort, R.J., 2003. Urocortin II treatment reduces skeletal muscle mass and function loss during atrophy and increases nonatrophying skeletal muscle mass and function. Endocrinology 144(11):4939–4946. https://doi.org/10.1210/en.2003-0271.

36 Gao, M.H., Giamouridis, D., Lai, N.C., Walenta, E., Paschoal, V.A., Kim, Y.C., et al., 2016. One-time injection of AAV8 encoding urocortin 2 provides long-term resolution of insulin resistance. JCI Insight 1(15):e88322. https://doi.org/10.1172/jci.insight.88322.

37 Bale, T.L., Anderson, K.R., Roberts, A.J., Lee, K.F., Nagy, T.R., Vale, W.W., 2003. Corticotropin-releasing factor receptor-2-deficient mice display abnormal homeostatic responses to challenges of increased dietary fat and cold. Endocrinology 144(6):2580–2587. https://doi.org/10.1210/en.2002-0091.

38 Li, C., Chen, P., Vaughan, J., et al., 2003. Urocortin III is expressed in pancreatic beta-cells and stimulates insulin and glucagon secretion. Endocrinology 144(7):3216–3224. https://doi.org/10.1210/en.2002-0087.

39 Borg, M.L., Massart, J., Schonke, M., de Castro Barbosa, T., Guo, L., Wade, M., et al., 2019. Modified UCN2 peptide acts as an insulin sensitizer in skeletal muscle of obese mice. Diabetes 68(7):1403–1414. https://doi.org/10.2337/db18-1237.

